Cite as: D. Voiry *et al.*, *Science* 10.1126/science.aah3398 (2016).

High-quality graphene via microwave reduction of solution-exfoliated graphene oxide

Damien Voiry,[1]*† Jieun Yang,[1]† Jacob Kupferberg,[1] Raymond Fullon,[1] Calvin Lee,[1] Hu Young Jeong,[2] Hyeon Suk Shin,[3] Manish Chhowalla[1]‡

[1]Materials Science and Engineering, Rutgers University, 607 Taylor Road, Piscataway, NJ 08854, USA. [2]UNIST Central Research Facilities (UCRF) and School of Materials Science and Engineering, UNIST, Ulsan 689-798, Republic of Korea. [3]Department of Chemistry and Department of Energy Engineering, Low Dimensional Carbon Materials, Ulsan National Institute of Science and Technology (UNIST), Ulsan 689-798, Republic of Korea.

*Present address: Institut Européen des Membranes (I.E.M.), University of Montpellier, Place Eugène Bataillon, 34095 Montpellier, France.

†These authors contributed equally to this work.

‡Corresponding author. Email: manish1@rci.rutgers.edu

Efficient exfoliation of graphite in solutions to obtain high-quality graphene flakes is desirable for printable electronics, catalysis, energy storage, and composites. Graphite oxide with large lateral dimensions has an exfoliation yield of ~100% but it has not been possible to completely remove the oxygen functional groups so that the reduced form of graphene oxide (GO) remains a highly disordered material. Here, we report a simple, rapid method to reduce GO (rGO) into pristine graphene using 1- to 2-second pulses of microwaves. The excellent structural properties are translated into mobility values of > 1000 centimeter squared per volt per second in field effect transistors (FETs) with MW-rGO as the channel material and in exceptionally high activity for MW-rGO catalyst support toward oxygen evolution reaction (OER).

Low yields of single-layered graphene, submicron lateral dimensions, and poor electronic properties remain as major challenges for solution exfoliated graphene flakes (*1*–*4*). Oxidation of graphite and its subsequent exfoliation into monolayered graphene oxide (GO) with large lateral dimensions (*5*–*7*) has an exfoliation yield of ~100% but despite numerous efforts, it has not been possible to completely remove the oxygen functional groups (*1*, *2*, *8*, *9*) so that the reduced form of GO (rGO) remains a highly disordered material with properties that are generally far inferior to chemical vapor deposited (CVD) graphene (*5*). Although rGO has been widely demonstrated to be potentially useful material for catalysis (*10*–*13*) and energy storage (*14*–*18*), even in its disordered form, efficient reduction of GO into high-quality graphene should lead to substantial enhancement in performance. Here, we report a simple and rapid method to reduce GO into pristine graphene using 1- to 2-s long pulses of microwaves. The microwave-reduced GO (MW-rGO) exhibits pristine CVD graphene-like features in the Raman spectrum with sharp G and 2D peaks and nearly absent D peak. X-ray photoelectron spectroscopy (XPS) and high-resolution transmission microscopy (HR-TEM) suggest highly ordered structure in which oxygen functional groups are almost entirely removed. The excellent structural properties are translated into mobility values of ~1500 cm^2-V^{-1}-s^{-1} in field effect transistors (FETs) with MW-rGO as the channel material and in exceptionally low Tafel slope values of ~38 mV/decade for MW-rGO catalyst support for oxygen evolution reaction (OER). These results suggest that reduction of GO using microwaves is highly efficient and realizes the goal of achieving high-quality graphene with excellent properties by solution exfoliation.

We used the modified Hummers' method to oxidize graphite and solubilize it into monolayered graphene oxide flakes in water (*19*). The stable suspension of GO sheets in water allows them be reconstituted in several different forms such as thin films (*20*), bucky paper (*21*), or fibers (*22*, *23*). As-synthesized GO is electrically insulating because of the presence of oxygen functional groups that are covalently bonded with the carbon atoms (*2*). Substantial effort has been devoted to recover the conducting π-states of sp^2 bonded carbon atoms by removing oxygen functional groups via chemical (*1*, *24*, *25*) or thermal (*26*) reduction [even heating over 3000 K (*23*)]. By carefully tuning the reduction procedure, it is possible to realize interesting optical (*20*, *27*, *28*) and electronic properties (*27*) of rGO that are substantially different from those of pristine graphene because the evolution of the oxygen functional groups during reduction is accompanied by the formation of defects in the graphene basal plane (*29*). Specifically, nanoscopic holes occur through loss of carbon as CO or CO_2 (*30*) and rearrangement of the carbon atoms in the graphene basal plane leads to formation of Stone-Wales types of defects (*31*). In addition, oxygen functional groups form highly stable ether and car-

bonyl groups (*32*) that are difficult to remove so that rGO contains a residual oxygen concentration of 15 to 25 atomic percent (*32*). These factors render rGO a highly defective material with vast majority of papers reporting electronic mobility values on the order of 1 cm^2-V^{-1}-s^{-1} (*33*–*35*).

GO flakes with lateral dimensions as high as tens of micrometers are shown in Fig. 1A. We used microwaves from a conventional microwave oven operated at 1000 W for 1 to 2 s pulses to reduce GO [See section "Preparation of Microwave reduced graphene oxide (MW-rGO)" in supplementary materials] (*36*). Irradiation of GO with microwaves has been reported previously (*37*–*39*), but the reduction efficiency has been low and the rGO remains highly disordered as indicated by the presence of an intense and broad disorder D band and absence of the 2D band in Raman. We irradiated GO after deposition to achieve exceptionally high-quality rGO. We started by slightly reducing GO by thermal annealing prior to exposure to microwaves, which made it conducting so it could absorb microwaves. We infer that absorption of microwaves led to rapid heating of the GO (fig. S1) (*36*), causing desorption of oxygen functional groups as well as reordering of the graphene basal plane.

The XPS results (Fig. 1B) indicate that MW-rGO was substantially reduced with in plane oxygen concentration of ~4 atomic %, much lower that what is theoretically predicted for rGO after annealing to 1500 K (*32*). Approximately 3 atomic % of noncovalently bonded adsorbed oxygen was also found in MW-rGO, CVD graphene, and graphite powder indicated by the fits in Fig. 1B. The FWHM of the XPS peak is slightly higher in the case MW-rGO than for CVD graphene and bulk graphite, suggesting that small amount of disorder is still present. The Raman spectra of MW-rGO along with those of thermally reduced GO, CVD graphene, liquid exfoliated graphene, and HOPG for comparison are shown in Fig. 1C. MW-rGO exhibited highly ordered graphene-like Raman features with sharp and symmetrical 2D and G peaks and nearly absent D peak (fig. S2) (*36*). The Raman spectrum for the MW-rGO (Fig. 1C) more closely resembled that of CVD graphene than the broad and highly disordered spectrum of thermally reduced rGO or that of solution exfoliated graphene films where the 2D peak is weak and the disorder induced D peak is also visible. The Raman spectra of MW-rGO are also different from those of electrochemically exfoliated graphene, chemically reduced GO and microwave exfoliated graphene oxide (MEGO), all of which exhibit high D band and moderate or no 2D band (*25*, *37*, *40*–*42*). We have also extracted the I_{2D}/I_G Raman peak ratios as a function of the graphene domain sizes (See section "Raman spectroscopy of the graphene oxide and microwaved reduced graphene oxide" in supplementary materials) (*36*). We found that MW-rGO exhibits substantially higher I_{2D}/I_G ratios and larger graphene domain sizes than rGO and solution exfoliated flakes (Fig. 1D).

Raman spectroscopy gives structural information averaged over regions a few micrometers in diameter. We investigated local atomic structure using aberration corrected HRTEM (Fig. 2). Thermally reduced GO exhibited the well-known disordered structure with holes and oxygen functional groups on the surface (Fig. 2A). The MW-rGO exhibited highly ordered structure at the atomic scale (Fig. 2, B and C), suggesting that there is some reorganization of the carbon bonding during microwave reduction along with removal of oxygen facilitated by achieving exceptionally high temperatures.

To investigate whether the highly ordered structure of MW-rGO can be translated into useful properties, we implemented it as the channel in FETs and as catalyst support for the oxygen evolution reactions. The mobility values in graphene have been used as a parameter for assessing the quality of the material (*43*). To this end, several studies have reported high mobility values of rGO (100 to 1000 cm^2/V-s) (*40*, *42*) to demonstrate efficacy of various reduction treatments or synthesis procedures. However, mobility values alone cannot provide information about the structural integrity of the material. Previous reports on high mobility rGO are accompanied by Raman spectra containing large D bands and weak 2D bands along with oxygen concentration of 5 to 8%, suggesting substantial disorder. Thus, mobility values > ~1 cm^2/V-s have not been widely reproducible in rGO. Transfer characteristics of FETs from MW-rGO on SiO_2 (see methods for device fabrication procedure) are shown in Fig. 3A (*36*). Drain currents in the milliamps range can be measured. The electrical properties of thermally reduced GO FETs are also shown for comparison in Fig. 3A, which exhibit substantially lower current values. The absence of Dirac point in the case of rGO is attributed to the poorly reduced and highly disordered structure of the nanosheets. Additionally, the presence of adsorbates and oxygen impurities are known to dramatically shift the position of Dirac point and to modify the FET characteristics. The mobility values extracted from FET measurements were >1000 cm^2-V^{-1}-s^{-1} for holes and electrons in MW-rGO (Inset Fig. 3A, fig. S4) (*36*). FETs measured here consist of large channel dimensions so that transport of carriers occurs over numerous flakes. Despite this, exceptionally high mobility values were obtained in MW-rGO, suggesting that individual flakes have very good transport properties. Although we obtain exceptional mobilities, they should be interpreted with caution as the actual values can be strongly influenced extrinsic factors such as contact resistance and scattering by charged impurities (*44*).

Highly conducting carbon based electrodes that are electrochemically stable, are important for applications in catalysis and energy storage. Catalysts are typically loaded on

highly conducting substrates (working electrode) such as carbon cloth, glassy carbon or nickel foam. We investigated the properties of MW-rGO as catalyst support in oxygen evolution reaction by depositing Fe and Ni layered double hydroxide (LDH) on MW-rGO (See methods in supplementary information) (*36*). The OER properties of Fe-Ni LDH catalysts on MW-rGO, rGO, and glassy carbon electrodes (Fig. 3B) (See methods for the electrochemical measurements) show that the overpotential at which the reaction starts decreased to <200 mV and the current density rapidly increased when MW-rGO was used as the catalyst support (*36*). To obtain insight into surface chemistry mechanisms, we have extracted the Tafel slopes from measurements on different supports (Fig. 3C). The MW-rGO catalyst supports exhibit exceptionally low Tafel slopes of 38 mV/dec which may indicate that the reaction $MO + OH^- = MOOH + e^-$ is the rate-determining step (where M represents an active site on the catalyst surface) (*45*). The much higher Tafel slopes for glassy carbon and rGO electrodes of 170 mV/dec and 360 mV/dec, respectively, suggest limiting reactions are caused by adsorption of hydroxide ions ($M + OH^- = MOH + e^-$) because of the poor electrical coupling between the catalyst and support (*45*). The limited electrical coupling is highlighted by the inset in Fig. 3C, which shows that the impedance of the electrochemical circuit is substantially lowered when using MW-rGO, which allows the OER to proceed efficiently. Electrochemical stability of the catalysts and their supports is an important parameter in catalysis. The stability of MW-rGO supports (Fig. 3D) was maintained for more than 15 hours, in contrast with glassy carbon supports that degraded almost immediately after the reaction started. We have made similar measurements for the hydrogen evolution reaction (HER) and obtained exceptional performance for MW-rGO catalyst supports as well as very high stability for more than 100 hours (See section "Hydrogen evolution reaction measurements" in supplementary materials) (*36*).

REFERENCES AND NOTES

1. S. Park, R. S. Ruoff, Chemical methods for the production of graphenes. *Nat. Nanotechnol.* **4**, 217–224 (2009).doi:10.1038/nnano.2009.58 Medline
2. K. P. Loh, Q. Bao, P. K. Ang, J. Yang, The chemistry of graphene. *J. Mater. Chem.* **20**, 2277–2289 (2010). doi:10.1039/b920539j
3. K. R. Paton, E. Varrla, C. Backes, R. J. Smith, U. Khan, A. O'Neill, C. Boland, M. Lotya, O. M. Istrate, P. King, T. Higgins, S. Barwich, P. May, P. Puczkarski, I. Ahmed, M. Moebius, H. Pettersson, E. Long, J. Coelho, S. E. O'Brien, E. K. McGuire, B. M. Sanchez, G. S. Duesberg, N. McEvoy, T. J. Pennycook, C. Downing, A. Crossley, V. Nicolosi, J. N. Coleman, Scalable production of large quantities of defect-free few-layer graphene by shear exfoliation in liquids. *Nat. Mater.* **13**, 624–630 (2014).doi:10.1038/nmat3944 Medline
4. K. P. Loh, Q. Bao, G. Eda, M. Chhowalla, Graphene oxide as a chemically tunable platform for optical applications. *Nat. Chem.* **2**, 1015–1024 (2010).doi:10.1038/nchem.907 Medline
5. C.-Y. Su, Y. Xu, W. Zhang, J. Zhao, X. Tang, C.-H. Tsai, L.-J. Li, Electrical and spectroscopic characterizations of ultra-large reduced graphene oxide monolayers. *Chem. Mater.* **21**, 5674–5680 (2009). doi:10.1021/cm902182y
6. J. Zhao, S. Pei, W. Ren, L. Gao, H.-M. Cheng, Efficient preparation of large-area graphene oxide sheets for transparent conductive films. *ACS Nano* **4**, 5245–5252 (2010).doi:10.1021/nn1015506 Medline
7. Q. Zheng, W. H. Ip, X. Lin, N. Yousefi, K. K. Yeung, Z. Li, J.-K. Kim, Transparent conductive films consisting of ultralarge graphene sheets produced by Langmuir-Blodgett assembly. *ACS Nano* **5**, 6039–6051 (2011).doi:10.1021/nn2018683 Medline
8. I. Jung, D. A. Dikin, R. D. Piner, R. S. Ruoff, Tunable electrical conductivity of individual graphene oxide sheets reduced at "low" temperatures. *Nano Lett.* **8**, 4283–4287 (2008).doi:10.1021/nl8019938 Medline
9. K. Erickson, R. Erni, Z. Lee, N. Alem, W. Gannett, A. Zettl, Determination of the local chemical structure of graphene oxide and reduced graphene oxide. *Adv. Mater.* **22**, 4467–4472 (2010).doi:10.1002/adma.201000732 Medline
10. E. Yoo, T. Okata, T. Akita, M. Kohyama, J. Nakamura, I. Honma, Enhanced electrocatalytic activity of Pt subnanoclusters on graphene nanosheet surface. *Nano Lett.* **9**, 2255–2259 (2009).doi:10.1021/nl900397t Medline
11. Y. Liang, Y. Li, H. Wang, J. Zhou, J. Wang, T. Regier, H. Dai, Co_3O_4 nanocrystals on graphene as a synergistic catalyst for oxygen reduction reaction. *Nat. Mater.* **10**, 780–786 (2011).doi:10.1038/nmat3087 Medline
12. Y. Li, H. Wang, L. Xie, Y. Liang, G. Hong, H. Dai, MoS_2 nanoparticles grown on graphene: An advanced catalyst for the hydrogen evolution reaction. *J. Am. Chem. Soc.* **133**, 7296–7299 (2011).doi:10.1021/ja201269b Medline
13. J. Yang, D. Voiry, S. J. Ahn, D. Kang, A. Y. Kim, M. Chhowalla, H. S. Shin, Two-dimensional hybrid nanosheets of tungsten disulfide and reduced graphene oxide as catalysts for enhanced hydrogen evolution. *Angew. Chem. Int. Ed.* **52**, 13751–13754 (2013).doi:10.1002/anie.201307475 Medline
14. M. D. Stoller, S. Park, Y. Zhu, J. An, R. S. Ruoff, Graphene-based ultracapacitors. *Nano Lett.* **8**, 3498–3502 (2008).doi:10.1021/nl802558y Medline
15. J. G. Radich, P. V. Kamat, Origin of reduced graphene oxide enhancements in electrochemical energy storage. *ACS Catal.* **2**, 807–816 (2012). doi:10.1021/cs3001286
16. H. Wang, L.-F. Cui, Y. Yang, H. Sanchez Casalongue, J. T. Robinson, Y. Liang, Y. Cui, H. Dai, Mn_3O_4-graphene hybrid as a high-capacity anode material for lithium ion batteries. *J. Am. Chem. Soc.* **132**, 13978–13980 (2010).doi:10.1021/ja105296a Medline
17. H. Wang, Y. Yang, Y. Liang, J. T. Robinson, Y. Li, A. Jackson, Y. Cui, H. Dai, Graphene-wrapped sulfur particles as a rechargeable lithium-sulfur battery cathode material with high capacity and cycling stability. *Nano Lett.* **11**, 2644–2647 (2011).doi:10.1021/nl200658a Medline
18. G. Yu, L. Hu, M. Vosgueritchian, H. Wang, X. Xie, J. R. McDonough, X. Cui, Y. Cui, Z. Bao, Solution-processed graphene/MnO_2 nanostructured textiles for high-performance electrochemical capacitors. *Nano Lett.* **11**, 2905–2911 (2011).doi:10.1021/nl2013828 Medline
19. W. S. Hummers Jr., R. E. Offeman, Preparation of graphitic oxide. *J. Am. Chem. Soc.* **80**, 1339 (1958). doi:10.1021/ja01539a017
20. G. Eda, G. Fanchini, M. Chhowalla, Large-area ultrathin films of reduced graphene oxide as a transparent and flexible electronic material. *Nat. Nanotechnol.* **3**, 270–274 (2008).doi:10.1038/nnano.2008.83 Medline
21. D. A. Dikin, S. Stankovich, E. J. Zimney, R. D. Piner, G. H. B. Dommett, G. Evmenenko, S. T. Nguyen, R. S. Ruoff, Preparation and characterization of graphene oxide paper. *Nature* **448**, 457–460 (2007).doi:10.1038/nature06016 Medline
22. R. Cruz-Silva, A. Morelos-Gomez, H. I. Kim, H. K. Jang, F. Tristan, S. Vega-Diaz, L. P. Rajukumar, A. L. Elías, N. Perea-Lopez, J. Suhr, M. Endo, M. Terrones, Super-stretchable graphene oxide macroscopic fibers with outstanding knotability fabricated by dry film scrolling. *ACS Nano* **8**, 5959–5967 (2014).doi:10.1021/nn501098d Medline
23. G. Xin, T. Yao, H. Sun, S. M. Scott, D. Shao, G. Wang, J. Lian, Highly thermally conductive and mechanically strong graphene fibers. *Science* **349**, 1083–1087 (2015).doi:10.1126/science.aaa6502 Medline
24. S. Park, Y. Hu, J. O. Hwang, E.-S. Lee, L. B. Casabianca, W. Cai, J. R. Potts, H.-W. Ha, S. Chen, J. Oh, S. O. Kim, Y.-H. Kim, Y. Ishii, R. S. Ruoff, Chemical structures of hydrazine-treated graphene oxide and generation of aromatic nitrogen doping. *Nat. Commun.* **3**, 638 (2012).doi:10.1038/ncomms1643 Medline
25. I. K. Moon, J. Lee, R. S. Ruoff, H. Lee, Reduced graphene oxide by chemical graphitization. *Nat. Commun.* **1**, 73 (2010).doi:10.1038/ncomms1067 Medline
26. X. Li, G. Zhang, X. Bai, X. Sun, X. Wang, E. Wang, H. Dai, Highly conducting

graphene sheets and Langmuir-Blodgett films. *Nat. Nanotechnol.* **3**, 538–542 (2008).doi:10.1038/nnano.2008.210 Medline
27. G. Eda, Y.-Y. Lin, C. Mattevi, H. Yamaguchi, H.-A. Chen, I.-S. Chen, C.-W. Chen, M. Chhowalla, Blue photoluminescence from chemically derived graphene oxide. *Adv. Mater.* **22**, 505–509 (2010).doi:10.1002/adma.200901996 Medline
28. Z. Luo, P. M. Vora, E. J. Mele, A. T. C. Johnson, J. M. Kikkawa, Photoluminescence and band gap modulation in graphene oxide. *Appl. Phys. Lett.* **94**, 111909 (2009). doi:10.1063/1.3098358
29. D. R. Dreyer, S. Park, C. W. Bielawski, R. S. Ruoff, The chemistry of graphene oxide. *Chem. Soc. Rev.* **39**, 228–240 (2010).doi:10.1039/B917103G Medline
30. R. Larciprete, S. Fabris, T. Sun, P. Lacovig, A. Baraldi, S. Lizzit, Dual path mechanism in the thermal reduction of graphene oxide. *J. Am. Chem. Soc.* **133**, 17315–17321 (2011).doi:10.1021/ja205168x Medline
31. J. Kotakoski, A. V. Krasheninnikov, K. Nordlund, Energetics, structure, and long-range interaction of vacancy-type defects in carbon nanotubes: Atomistic simulations. *Phys. Rev. B* **74**, 245420 (2006). doi:10.1103/PhysRevB.74.245420
32. A. Bagri, C. Mattevi, M. Acik, Y. J. Chabal, M. Chhowalla, V. B. Shenoy, Structural evolution during the reduction of chemically derived graphene oxide. *Nat. Chem.* **2**, 581–587 (2010).doi:10.1038/nchem.686 Medline
33. Z. Luo, Y. Lu, L. A. Somers, A. T. C. Johnson, High yield preparation of macroscopic graphene oxide membranes. *J. Am. Chem. Soc.* **131**, 898–899 (2009).doi:10.1021/ja807934n Medline
34. H. A. Becerril, J. Mao, Z. Liu, R. M. Stoltenberg, Z. Bao, Y. Chen, Evaluation of solution-processed reduced graphene oxide films as transparent conductors. *ACS Nano* **2**, 463–470 (2008).doi:10.1021/nn700375n Medline
35. S. Wang, P. K. Ang, Z. Wang, A. L. L. Tang, J. T. L. Thong, K. P. Loh, High mobility, printable, and solution-processed graphene electronics. *Nano Lett.* **10**, 92–98 (2010).doi:10.1021/nl9028736 Medline
36. See supplementary materials.
37. Y. Zhu, S. Murali, M. D. Stoller, A. Velamakanni, R. D. Piner, R. S. Ruoff, Microwave assisted exfoliation and reduction of graphite oxide for ultracapacitors. *Carbon* **48**, 2118–2122 (2010). doi:10.1016/j.carbon.2010.02.001
38. W. Chen, L. Yan, P. R. Bangal, Preparation of graphene by the rapid and mild thermal reduction of graphene oxide induced by microwaves. *Carbon* **48**, 1146–1152 (2010). doi:10.1016/j.carbon.2009.11.037
39. H. Hu, Z. Zhao, Q. Zhou, Y. Gogotsi, J. Qiu, The role of microwave absorption on formation of graphene from graphite oxide. *Carbon* **50**, 3267–3273 (2012). doi:10.1016/j.carbon.2011.12.005
40. H. Feng, R. Cheng, X. Zhao, X. Duan, J. Li, A low-temperature method to produce highly reduced graphene oxide. *Nat. Commun.* **4**, 1539 (2013).doi:10.1038/ncomms2555 Medline
41. K. Parvez, Z.-S. Wu, R. Li, X. Liu, R. Graf, X. Feng, K. Müllen, Exfoliation of graphite into graphene in aqueous solutions of inorganic salts. *J. Am. Chem. Soc.* **136**, 6083–6091 (2014).doi:10.1021/ja5017156 Medline
42. S. Eigler, M. Enzelberger-Heim, S. Grimm, P. Hofmann, W. Kroener, A. Geworski, C. Dotzer, M. Röckert, J. Xiao, C. Papp, O. Lytken, H.-P. Steinrück, P. Müller, A. Hirsch, Wet chemical synthesis of graphene. *Adv. Mater.* **25**, 3583–3587 (2013).doi:10.1002/adma.201300155 Medline
43. N. Petrone, C. R. Dean, I. Meric, A. M. van der Zande, P. Y. Huang, L. Wang, D. Muller, K. L. Shepard, J. Hone, Chemical vapor deposition-derived graphene with electrical performance of exfoliated graphene. *Nano Lett.* **12**, 2751–2756 (2012).doi:10.1021/nl204481s Medline
44. I. McCulloch, A. Salleo, M. Chabinyc, Avoid the kinks when measuring mobility. *Science* **352**, 1521–1522 (2016).doi:10.1126/science.aaf9062 Medline
45. T. Shinagawa, A. T. Garcia-Esparza, K. Takanabe, Insight on Tafel slopes from a microkinetic analysis of aqueous electrocatalysis for energy conversion. *Sci. Rep.* **5**, 13801 (2015).doi:10.1038/srep13801 Medline
46. X. Li, C. W. Magnuson, A. Venugopal, J. An, J. W. Suk, B. Han, M. Borysiak, W. Cai, A. Velamakanni, Y. Zhu, L. Fu, E. M. Vogel, E. Voelkl, L. Colombo, R. S. Ruoff, Graphene films with large domain size by a two-step chemical vapor deposition process. *Nano Lett.* **10**, 4328–4334 (2010).doi:10.1021/nl101629g Medline
47. M. S. Dresselhaus, A. Jorio, M. Hofmann, G. Dresselhaus, R. Saito, Perspectives on carbon nanotubes and graphene Raman spectroscopy. *Nano Lett.* **10**, 751–758 (2010).doi:10.1021/nl904286r Medline
48. A. C. Ferrari, J. C. Meyer, V. Scardaci, C. Casiraghi, M. Lazzeri, F. Mauri, S. Piscanec, D. Jiang, K. S. Novoselov, S. Roth, A. K. Geim, Raman spectrum of graphene and graphene layers. *Phys. Rev. Lett.* **97**, 187401 (2006).doi:10.1103/PhysRevLett.97.187401 Medline
49. A. C. Ferrari, D. M. Basko, Raman spectroscopy as a versatile tool for studying the properties of graphene. *Nat. Nanotechnol.* **8**, 235–246 (2013).doi:10.1038/nnano.2013.46 Medline
50. L. G. Cançado, A. Jorio, E. H. M. Ferreira, F. Stavale, C. A. Achete, R. B. Capaz, M. V. O. Moutinho, A. Lombardo, T. S. Kulmala, A. C. Ferrari, Quantifying defects in graphene via Raman spectroscopy at different excitation energies. *Nano Lett.* **11**, 3190–3196 (2011).doi:10.1021/nl201432g Medline
51. L. G. Cançado, K. Takai, T. Enoki, M. Endo, Y. A. Kim, H. Mizusaki, A. Jorio, L. N. Coelho, R. Magalhães-Paniago, M. A. Pimenta, General equation for the determination of the crystallite size L_a of nanographite by Raman spectroscopy. *Appl. Phys. Lett.* **88**, 163106 (2006). doi:10.1063/1.2196057
52. S. Stankovich, D. A. Dikin, R. D. Piner, K. A. Kohlhaas, A. Kleinhammes, Y. Jia, Y. Wu, S. B. T. Nguyen, R. S. Ruoff, Synthesis of graphene-based nanosheets via chemical reduction of exfoliated graphite oxide. *Carbon* **45**, 1558–1565 (2007). doi:10.1016/j.carbon.2007.02.034
53. J. Zhang, H. Yang, G. Shen, P. Cheng, J. Zhang, S. Guo, Reduction of graphene oxide via L-ascorbic acid. *Chem. Commun.* **46**, 1112–1114 (2010).doi:10.1039/B917705A Medline
54. C. Mattevi, G. Eda, S. Agnoli, S. Miller, K. A. Mkhoyan, O. Celik, D. Mastrogiovanni, G. Granozzi, E. Garfunkel, M. Chhowalla, Evolution of electrical, chemical, and structural properties of transparent and conducting chemically derived graphene thin films. *Adv. Funct. Mater.* **19**, 2577–2583 (2009). doi:10.1002/adfm.200900166
55. F. Chen, Q. Qing, J. Xia, J. Li, N. Tao, Electrochemical gate-controlled charge transport in graphene in ionic liquid and aqueous solution. *J. Am. Chem. Soc.* **131**, 9908–9909 (2009).doi:10.1021/ja9041862 Medline
56. S.-K. Lee, B. J. Kim, H. Jang, S. C. Yoon, C. Lee, B. H. Hong, J. A. Rogers, J. H. Cho, J.-H. Ahn, Stretchable graphene transistors with printed dielectrics and gate electrodes. *Nano Lett.* **11**, 4642–4646 (2011).doi:10.1021/nl202134z Medline
57. X. Lu, C. Zhao, Electrodeposition of hierarchically structured three-dimensional nickel-iron electrodes for efficient oxygen evolution at high current densities. *Nat. Commun.* **6**, 6616 (2015).doi:10.1038/ncomms7616 Medline

ACKNOWLEDGMENTS

M.C. and D.V. acknowledge financial support from NSF DGE 0903661 and ECCS 1128335. J.Y., J.K., and M.C. acknowledge financial support from the Rutgers Energy Institute. R.F. acknowledge financial support from the US Dept. of Education GAANN Grant number P200A120142. C.L. and J.K. acknowledge support from the Rutgers ARESTY Research Assistant program. H.S.S acknowledges NRF grant (No. NRF 2014R1A2A2A01007136) and a grant (Code No. 2011-0031630) from the Center for Advanced Soft Electronics under the Global Frontier Research Program through the National Research Foundation funded by the Ministry of Science, ICT and Future Planning, Korea. All data are in the print paper and online supplement.

SUPPLEMENTARY MATERIALS

www.sciencemag.org/cgi/content/full/science.aah3398/DC1
Materials and Methods
Supplementary Text
Figs. S1 to S6
Table S1
References (*46*–*57*)

12 June 2016; resubmitted 27 July 2016
Accepted 23 August 2016
Published online 1 September 2016
10.1126/science.aah3398

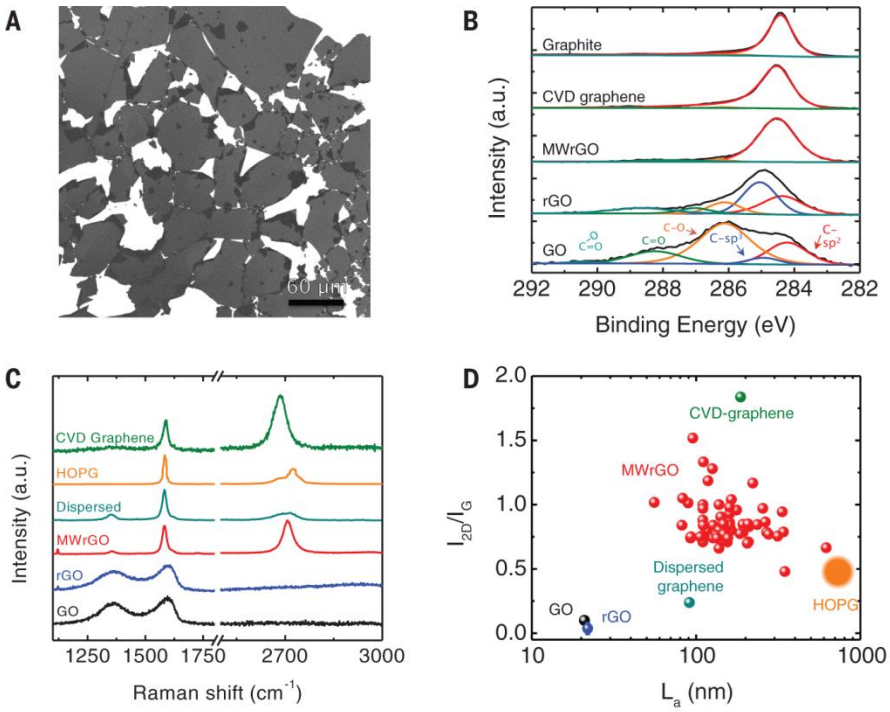

Fig. 1. Physical characterization of microwaved reduced graphene oxide (MW-rGO) compared to pristine graphene oxide (GO), reduced graphene oxide (rGO) and CVD-grown graphene (CVD graphene). (**A**) Scanning electron microscopy (SEM) of the single-layer graphene oxide flakes deposited on a silicon wafer. Graphene oxide nanosheets typically have lateral dimension of ~50 µm. (**B**) High-resolution x-ray photoelectron spectra from the C1s regions for microwaved reduced graphene oxide (MW-rGO) compared to pristine graphene oxide (GO), reduced graphene oxide (rGO), CVD-grown graphene and graphite. Each spectrum can be deconvoluted with components from the carbon-carbon bonds (sp^3: C-C and sp^2: C=C) as well oxygen functional groups (C-O, C=O and C-O=O) allowing the quantification of the oxygen content. (**C**) Raman spectra of MW-rGO and other graphene-based samples. Spectrum obtained for MW-rGO is similar to the spectrum of CVD graphene with the presence of a high and symmetrical 2D band together with a minimal D band. Sharp Raman peaks indicate high crystallinity of MW-rGO and demonstrate the quality of microwave reduction. (**D**) Evolution of the I_{2D}/I_G vs. the crystal size (L_a) for MW-rGO, GO, rGO, highly ordered pyrolytic graphite (HOPG), dispersed graphene and graphene from Ref (*3*). 62 measurements on different (~5) MW-rGO samples are reported. I_{2D}/I_G and L_a values for MW-rGO are approaching those of graphene and are significantly higher than rGO and dispersed graphene.

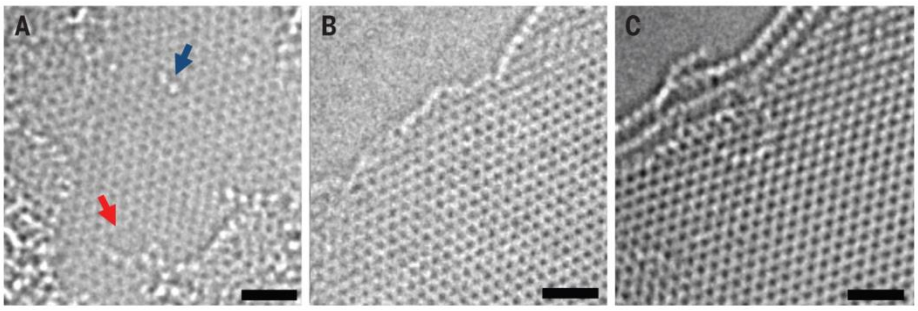

Fig. 2. High-resolution transmission electron microscopy (HR-TEM) of MW-rGO nanosheets. (**A**) HR-TEM of single-layer rGO presenting high density of defects: holes (red arrow) and oxygen functional groups (blue arrow). Bi-layer (**B**) and Tri-layer (**C**) HR-TEM of MW-rGO showing highly ordered structure. Scale bar = 1 nm.

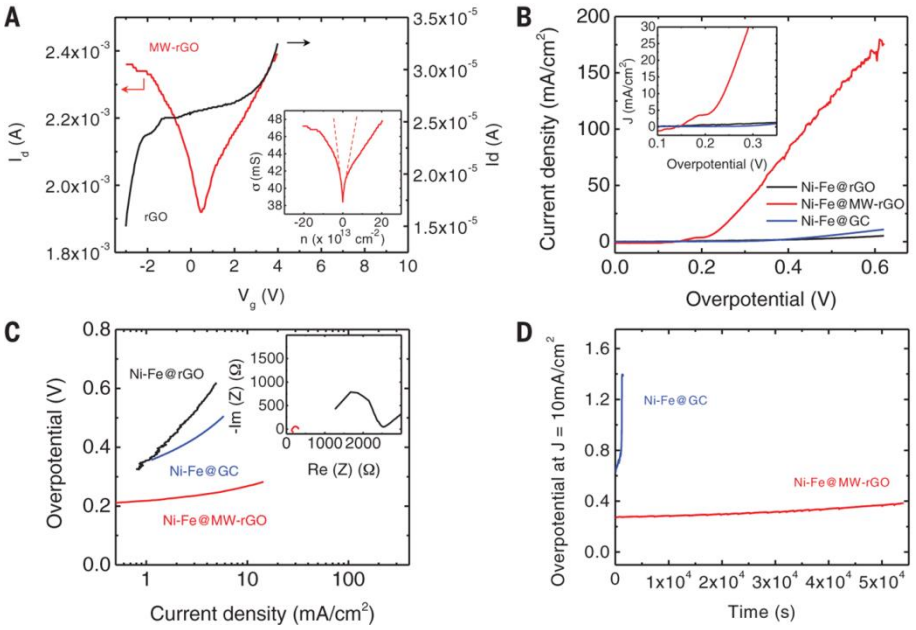

Fig. 3. Characterization of the electronic and electrocatalytic properties of MW-rGO. (**A**) Transfer characteristics of MW-rGO and rGO measured at V_{ds} = 50 mV. MW-rGO displays ambipolar behavior with a Dirac cone at V_g ~ 0.5 V. Inset: Evolution of the MW-rGO conductivity with the carrier density. (**B**) Polarization curves obtained from Ni-Fe layered double hydroxide (LDH) deposited on MW-rGO (Ni-Fe@MW-rGO), rGO (Ni-Fe@rGO) and glassy carbon (Ni-Fe@GC). Inset shows the magnification of the onset potential. (**C**) Tafel plot of Ni-Fe LDH deposited on MW-rGO compared to GC and rGO. Inset: Nyquist plots of the different samples obtained by electrochemical impedance spectroscopy at η = 200 mV. Ni-Fe@MW-rGO clearly shows a reduced internal resistance and minimal charge transfer resistance attributed to the high conductivity of the MW-rGO nanosheets. (**D**) Galvanostatic measurements showing the electrocatalytic stability of Ni-Fe LDH deposited on glassy carbon and MW-rGO when driving a 10 mA/cm^2 current density over 15 hours. MW-rGO support shows the best stability with minimal change of the overpotential. At the opposite, the activity from Ni-Fe LDH on glassy carbon decreases rapidly.

High-quality graphene via microwave reduction of solution-exfoliated graphene oxide

Damien Voiry, Jieun Yang, Jacob Kupferberg, Raymond Fullon, Calvin Lee, Hu Young Jeong, Hyeon Suk Shin and Manish Chhowalla

(September 1, 2016)
published online September 1, 2016

Editor's Summary

Science (print ISSN 0036-8075; online ISSN 1095-9203) is published weekly, except the last week in December, by the American Association for the Advancement of Science, 1200 New York Avenue NW, Washington, DC 20005.